J|A|C|S
ARTICLES
Published on Web 04/19/2006

Cope Elimination: Elucidation of Solvent Effects from QM/MM Simulations

Orlando Acevedo and William L. Jorgensen*

Contribution from the Department of Chemistry, Yale University, 225 Prospect Street, New Haven, Connecticut 06520-8107.

Received November 3, 2005; E-mail: william.jorgensen@yale.edu

Abstract: The Cope elimination reactions for *threo*- and *erythro*-*N*,*N*-dimethyl-3-phenyl-2-butylamine oxide have been investigated using QM/MM calculations in water, THF, and DMSO. The aprotic solvents provide up to million-fold rate accelerations. The effects of solvation on the reactants, transition structures, and rates of reaction are elucidated here using two-dimensional potentials of mean force (PMF) derived from free-energy perturbation calculations in Monte Carlo simulations (MC/FEP). The resultant free energies of activation in solution are in close agreement with experiment. Ab initio calculations at the MP2/6-311+G(2d,p) level using the PCM continuum solvent model were also carried out; however, only the QM/MM methodology was able to reproduce the large rate increases in proceeding from water to the dipolar aprotic solvents. Solute−solvent interaction energies and radial distribution functions are also analyzed and show that poorer solvation of the reactant in the aprotic solvents is primarily responsible for the observed rate enhancements. It is found that the amine oxide oxygen is the acceptor of three hydrogen bonds from water molecules for the reactant but only one to two weaker ones at the transition state. The overall quantitative success of the computations supports the present QM/MM/MC approach, featuring PDDG/PM3 as the QM method.

Introduction

The Cope elimination of amine oxides is valuable for the stereospecific synthesis of olefins (Scheme 1).[1] The reaction is extraordinarily sensitive to solvent effects; million-fold rate increases can be obtained in going from protic to aprotic solvents.[2,3] Even among aprotic solvents increasing polarity significantly reduces the reaction rate. The mechanism features a syn periplanar elimination based on stereochemical[2−4] and isotopic-labeling experiments.[5] Deviations from coplanarity are energetically unfavorable. Thus, cyclohexylamine oxides are unreactive due to atom staggering, while reactivity is restored for 7−10-membered rings, which have enough flexibility to allow the necessary eclipsing without excessive strain.[6] In addition to solvent effects, substituent effects can also be significant, e.g., replacement of a β-ethyl group by β-phenyl provides a 100-fold rate increase.[6] This observation is in line with the importance of breaking the carbon−hydrogen bond in proceeding to the transition state.

Scheme 1. Decomposition of *threo*- and *erythro*-*N*,*N*-Dimethyl-3-phenyl-2-butylamine Oxide

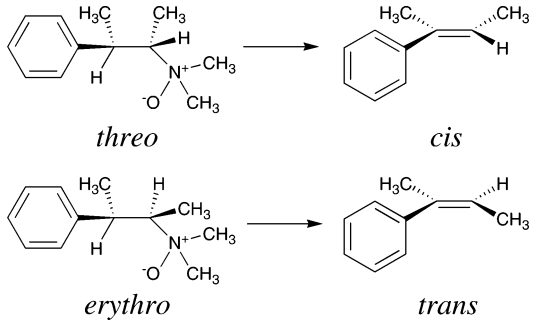

To elucidate these dramatic kinetic effects at the atomic level, mixed quantum and molecular mechanical (QM/MM) simulations have been carried out on the oxides of *threo*- and *erythro*-*N*,*N*-dimethyl-3-phenyl-2-butylamine, which give predominantly *cis*- and *trans*-2-phenyl-2-butene as products,[2a] respectively, (Scheme 1) with one side product, 3-phenyl-1-butene, in small amounts. These amine oxides were chosen to enable direct comparison of the present results with those from the extensive experimental study by Sahyun and Cram.[3] Reactants and transition structures have been located in three different solvents: water, DMSO, and THF; activation barriers were computed with complete sampling of the geometry of the reacting systems and explicit representation of the solvent molecules. Changes in solvation along the reaction paths are fully characterized. Prior knowledge on the origin of solvent effects for such reactions of amine oxides is limited. In the

(1) (a) Cope, A. C.; Foster, T. T.; Towie, P. H. *J. Am. Chem. Soc.* **1949**, *71*, 3929−3934. (b) Cope, A. C.; Trumbull, E. R. In *Organic Reactions*; John Wiley and Sons: New York, 1960; Vol. 11, pp 317−487.
(2) (a) Cram, D. J.; McCarty, J. E. *J. Am. Chem. Soc.* **1954**, *76*, 5740−5745. (b) Cram, D. J.; Sahyun, M. R. *J. Am. Chem. Soc.* **1962**, *84*, 1734−1735.
(3) Sahyun, M. R.; Cram, D. J. *J. Am. Chem. Soc.* **1963**, *85*, 1263−1268.
(4) (a) Cope, A. C.; LeBel, N. A. *J. Am. Chem. Soc.* **1960**, *82*, 4656−4662. (b) Saunders, W. H.; Cockerill, A. F. *Mechanisms of Elimination Reactions*; Wiley-Interscience: New York, 1973.
(5) (a) Bach, R. D.; Andrezejewski, D.; Dusold, L. R. *J. Org. Chem.* **1973**, *34*, 1742−1743. (b) Bach, R. D.; Braden, M. L. *J. Org. Chem.* **1991**, *56*, 7194−7195. (c) Bach, R. D.; Gonzalez, C.; Andres, J. L.; Schlegel, H. B. *J. Org. Chem.* **1995**, *60*, 4653−4656.
(6) DePuy, C. H.; King, R. W. *Chem. Rev.* **1960**, *60*, 431−457.

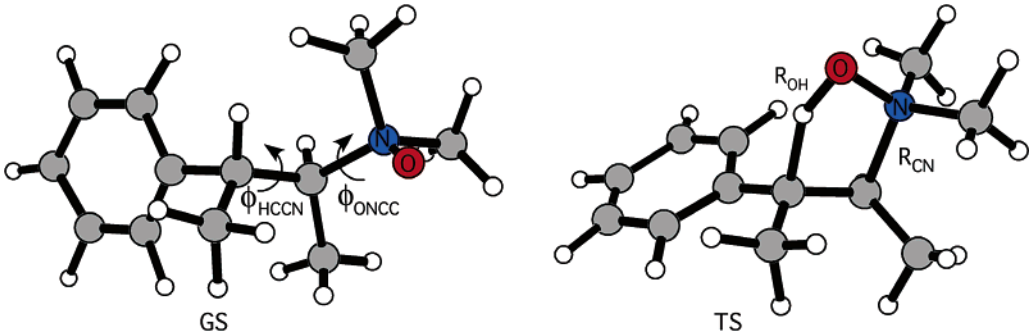

Figure 1. Dihedral variables, ϕ_{HCCN} and ϕ_{ONCC}, and bond length variables, R_{OH} and R_{CN}, for the Cope eliminations of *threo*- and *erythro*-*N*,*N*-dimethyl-3-phenyl-2-butylamine oxide. Illustrated structures are for the threo ground state (GS) and transition state (TS) from QM/MM simulations in THF using PDDG/PM3.

absence of the experimental data of Cram and co-workers,[2,3] expectations for the magnitude of the solvent effects are unclear. This is well illustrated by the recent joint computational and experimental study of the Meisenheimer rearrangement of an *N*-propargylamine oxide.[7] The Meisenheimer rearrangement and Cope elimination can be categorized as closely analogous examples of six-electron, pericyclic [2,3]-shifts of amine oxides. It was stated that the fact that the Meisenheimer rearrangements "involving a pericyclic rate-determining step, exhibit a significant solvent dependence was unexpected."[7]

Computational Methods

Mixed QM/MM calculations,[8] as implemented in BOSS 4.6,[9] were carried out with the reacting system treated using the semiempirical PDDG/PM3 method.[10] PDDG/PM3 has been extensively tested for gas-phase structures and energetics[10] and has given excellent results in solution-phase QM/MM studies of S_N2 reactions,[11] a nucleophilic aromatic substitution (S_NAr),[12] and Kemp decarboxylations of 3-carboxybenzisoxazoles.[13] The solvent molecules are represented with the united-atom OPLS force field[14] for the nonaqueous solvents and with the TIP4P water model.[15] The systems consisted of the reactants, plus 395 solvent molecules for the nonaqueous solvents, or 740 molecules for water. The systems are periodic and tetragonal with $c/a = 1.5$; a is ca. 25, 31, and 33 Å for water, DMSO, and THF. To locate the minima and maxima on the free-energy surface, two-dimensional free-energy maps were constructed for each reaction. Free-energy perturbation (FEP) calculations were performed in conjunction with NPT Metropolis Monte Carlo (MC) simulations at 25 °C and 1 atm. In this QM/MM implementation, the solute intramolecular energy is treated quantum mechanically using PDDG/PM3; computation of the QM energy and atomic charges is performed for every attempted solute move, occurring every 100 configurations. For electrostatic contributions to the solute−solvent energy, CM3 charges[16] obtained for the solute in the PDDG/PM3 calculations were used with a scale factor of 1.14.[17] This combination is appropriate for a PM3-based method, and it minimizes errors in computed free energies of hydration.[17] Solute−solvent and solvent−solvent intermolecular cutoff distances of 12 Å were employed based roughly on center-of-mass separations.

Density functional theory (DFT), specifically, B3LYP[18] with the 6-31G(d) basis set, was also used to characterize the transition structures and ground states in vacuum using Gaussian 03.[19] Electron correlation has been shown to be significant in describing the electronics of similar Cope eliminations.[6,20] The B3LYP/6-31G(d) calculations were used for geometry optimizations and computations of vibrational frequencies, which confirmed all stationary points as either minima or transition structures and provided thermodynamic and zero-point energy corrections. The effect of solvent was approximated by subsequent single-point calculations using the polarizable continuum model (PCM)[21] with a larger basis set, 6-311+G(2d,p); dielectric constants of 78.39, 46.7, and 7.58 were used for water, DMSO, and THF.

Results and Discussion

Energetics and Structure. Ground-state geometries for the amine oxides in solution were located with the MC/FEP calculations starting from gas-phase PDDG/PM3 structures and perturbing the central HCCN and CCNO dihedral angles in increments of 0.5°, as shown in Figure 1. The free energies of activation were calculated by perturbing to and then locking both dihedral angles at 0°, as a five-membered cyclic transition structure has been supported both experimentally[3] and theoretically,[6,20] and then by perturbing the distances between oxygen and the reacting hydrogen of the amine oxide (R_{OH}) and between the nitrogen and carbon (R_{CN}) to find the transition structures. All internal degrees of freedom other than the reaction coordinates were fully sampled during the MC/FEP calculations.

The initial ranges for R_{CN} and R_{OH} were 1.5−2.5 Å and 0.95−1.85 Å, respectively, with an increment of 0.05 Å. Each FEP

(7) Musci, Z.; Szabó, A.; Hermecz, I.; Kucsman, A.; Csizmadia, I. G. *J. Am. Chem. Soc.* **2005**, *127*, 7615−7631.
(8) (a) Åqvist, J.; Warshel, A. *Chem. Rev.* **1993**, *93*, 2523−2544. (b) Gao, J. *Acc. Chem. Res.* **1996**, *29*, 298−305. (c) Kaminski, G. A.; Jorgensen, W. L. *J. Phys. Chem. B* **1998**, *102*, 1787−1796.
(9) Jorgensen, W. L.; Tirado-Rives, J. *J. Comput. Chem.* **2005**, *26*, 1689−1700.
(10) (a) Repasky, M. P.; Chandrasekhar, J.; Jorgensen, W. L. *J. Comput. Chem.* **2002**, *23*, 1601−1622. (b) Tubert-Brohman, I.; Guimarães, C. R. W.; Repasky, M. P.; Jorgensen, W. L. *J. Comput. Chem.* **2003**, *25*, 138−150. (c) Tubert-Brohman, I.; Guimarães, C. R. W.; Jorgensen, W. L. *J. Chem. Theory Comput.* **2005**, *1*, 817−823.
(11) Vayner, G.; Houk, K. N.; Jorgensen, W. L.; Brauman, J. I. *J. Am. Chem. Soc.* **2004**, *126*, 9054−9058.
(12) Acevedo, O.; Jorgensen, W. L. *Org. Lett.* **2004**, *6*, 2881−2884.
(13) Acevedo, O.; Jorgensen, W. L. *J. Am. Chem. Soc.* **2005**, *127*, 8829−8834.
(14) (a) Jorgensen, W. L.; Briggs, J. M.; Contreras, M. L. *J. Phys. Chem.* **1990**, *94*, 1683−1686. (b) Briggs, J. M.; Matsui, T.; Jorgensen, W. L. *J. Comput. Chem.* **1990**, *11*, 958−971. (c) Jorgensen, W. L.; Briggs, J. M. *Mol. Phys.* **1988**, *63*, 547−558.
(15) Jorgensen, W. L.; Chandrasekhar, J.; Madura, J. D.; Impey, W.; Klein, M. L. *J. Chem. Phys.* **1983**, *79*, 926−935.
(16) Thompson, J. D.; Cramer, C. J.; Truhlar, D. G. *J. Comput. Chem.* **2003**, *24*, 1291−1304.
(17) Udier-Blagovic, M.; Morales de Tirado, P.; Pearlman, S. A.; Jorgensen, W. L. *J. Comput. Chem.* **2004**, *25*, 1322−1332.
(18) (a) Becke, A. D. *J. Chem. Phys.* **1993**, *98*, 5648−5652. (b) Lee, C.; Yang, W.; Parr, R. G. *Phys. Rev.* **1988**, *37*, 785−789.
(19) Frisch, M. J.; et al. *Gaussian 03*, revision A.1; Gaussian, Inc.: Pittsburgh, PA, 2003 full reference given in the Supporting Information.
(20) Komaromi, I.; Tronchet, J. M. J. *J. Phys. Chem. A* **1997**, *101*, 3554−3560.
(21) Tomasi, J.; Persico, M. *Chem. Rev.* **1994**, *94*, 2027−2094.

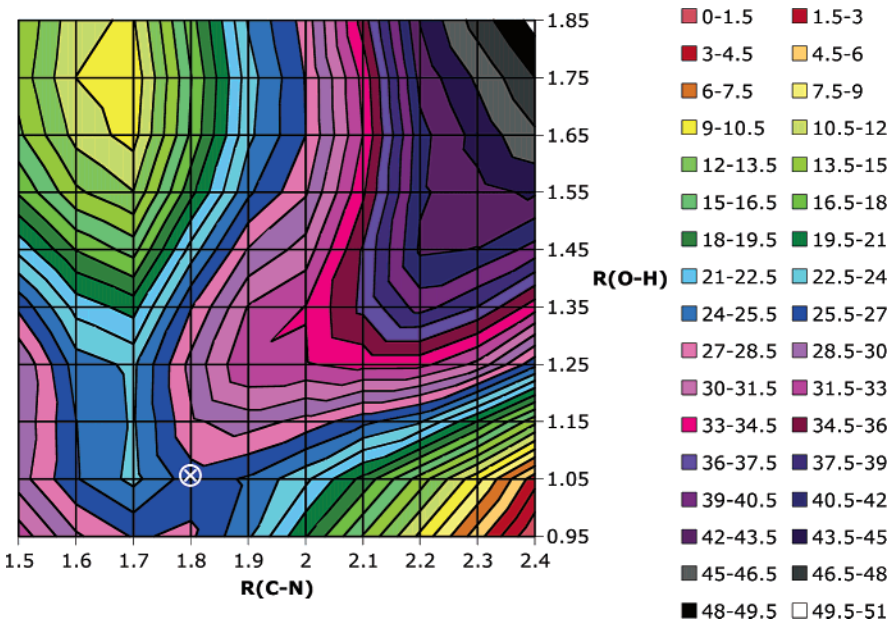

Figure 2. Two-dimensional potential of mean force (free-energy map) for the erythro amine oxide Cope elimination in DMSO; ⊗ indicates the location of the saddle point that represents the solution-phase transition structure. All distances are in angstroms, and relative free energy is in kcal/mol.

Table 1. Computed Bond Lengths (Å) for the threo and erythro Amine Oxide Transition Structures at 25 °C and 1 atm[a]

	gas[b]	water[c]	DMSO[c]	THF[c]
		threo		
R_{OH}	1.14	1.05	1.02	1.04
R_{CN}	1.65	1.82	1.75	1.73
R_{CH}	1.49	1.60	1.63	1.60
R_{CC}	1.49	1.46	1.46	1.46
R_{NO}	1.36	1.39	1.39	1.37
		erythro		
R_{OH}	1.12	1.02	1.05	1.03
R_{CN}	1.67	1.82	1.77	1.74
R_{CH}	1.51	1.67	1.63	1.61
R_{CC}	1.48	1.42	1.46	1.46
R_{NO}	1.36	1.42	1.38	1.39

[a] R_{CH}, R_{CC}, and R_{NO} are average distances for 10 M configurations in solution. [b] From PDDG/PM3 optimizations. [c] From the 2D free-energy maps computed in the MC/FEP simulations.

Table 2. Free Energies of Activation, $\Delta G^{\ddagger}$ (kcal/mol), at 25 °C for the Cope Elimination of *threo*- and e*rythro*-*N*,*N*-Dimethyl-3-phenyl-2-butyl-amine Oxide from QM/MM/MC Simulations

	R[a]	Φ[a]	$\Delta G^{\ddagger}$	exptl[b]
		threo		
water	27.3	10.9	38.1	31.1[c]
DMSO	17.2	8.7	25.9	23.5
THF	16.2	7.5	23.7	22.2
		erythro		
water	24.6	9.7	34.3	31.8[d]
DMSO	15.5	6.5	22.0	24.2
THF	15.8	6.2	22.0	23.1

[a] *R* and Φ are the separate bond rearrangement and torsional contributions. [b] Reference 3. [c] 132 °C. [d] 138 °C.

calculation entailed 2.5−5 M configurations of equilibration followed by 5−10 M configurations of averaging. As an example, the resultant map for the erythro isomer in DMSO, which required ca. 200 FEP calculations, is shown in Figure 2. In all cases, the transition structures and reactant states were readily located. The number of single-point QM calculations to construct one such map was ca. 15 million for the dihedral-angle mapping and 17 million for the bond perturbations, clearly showing the need for highly efficient QM methods in such studies.

To locate the critical points more precisely, the regions surrounding the free-energy minima and maxima from the initial maps were explored using increments of 0.01 Å. This provided refined results for the threo and erythro eliminations in the three solvents, as summarized in Table 1. The geometries show that for the five atoms participating directly in the reactions (H−C−C−N=O → C=C N−O−H), the protic solvent gives a marginally later transition structure with the double bond at 1.42−1.46 Å and with a longer R_{CN} distance at 1.82 Å. In the aprotic solvents the emerging double bond is similarly formed (1.46 Å), but the C−N bond is less advanced at 1.73−1.77 (Table 1). In all cases, the O−H bond is nearly completely formed at the solvated transition structures with R_{OH} = 1.02−1.05 Å, while in the gas-phase R_{OH} = 1.12−1.14 Å. The length of the breaking C−H bond in the transition structures is 1.60−1.67 Å in solution.

The computed activation barriers for the elimination of the threo and erythro amine oxides are summarized in Table 2; contributions to the activation barrier result from the separate FEP calculations for the torsional change to achieve the syn periplanar geometry (Φ) and the bond perturbations (*R*). Uncertainties in the free-energy barriers are calculated by propagating the standard deviation (σ_i) on the individual ΔG_i values. Smooth free-energy profiles were obtained with statistical uncertainties (1σ) of only 0.01−0.04 kcal/mol in each window; thus the overall uncertainties in the computed free energies of activation, $\Delta G^{\ddagger}$, are below 0.7 kcal/mol ($0.04^2 \times 320$ windows)$^{1/2}$. The computed $\Delta G^{\ddagger}$ values reproduce well the large rate enhancements in progressing from water to the aprotic solvents. The quantitative accord with experiment is particularly good for the aprotic solvents, though the slightly higher barriers for the erythro isomer are not reproduced. For reference, the gas-phase enthalpies of activation for the threo and erythro eliminations are 22.4 and 24.5 kcal/mol from PDDG/PM3, so the ordering inverted in the MC/FEP calculations.

Table 3. DFT and MP2 Results for $\Delta G^{\ddagger}$ (kcal/mol), at 25 °C for the Cope Eliminations[a]

	gas	water[b]	DMSO[b]	THF[b]
		threo		
B3LYP	12.3	18.6	18.3	17.1
MP2	16.9	24.5	24.1	22.7
exptl[c]		31.1	23.5	22.2
		erythro		
B3LYP	11.6	18.8	18.5	17.3
MP2	16.0	24.8	24.4	22.9
exptl[c]		31.8	24.2	23.1

[a] Using the 6-311+G(2d,p) basis set with B3LYP/6-31G(d) optimized geometries and vibrational frequencies. [b] PCM results. [c] Reference 3.

Previous theoretical work on the Cope elimination has been carried out by Komaromi and Tronchet on the simplest system yielding ethylene and hydroxylamine.[20] The computed activation energies were found to be highly dependent on the theoretical method. In the gas phase, the highest-energy barriers were obtained with Hartree−Fock (HF) calculations, while DFT gave the lowest; Møller−Plesset theory (MP2) gave results more in line with experimental data.[20] Solvation was investigated using HF/6-31G(d,p) and the Onsager continuum model with a range of dielectric constants; very little variation in the activation energies was found in contrast to experiment. For dielectric constants of 80, 40, and 10 (comparable to water, DMSO, and THF) the calculated activation energies were 44.8, 44.8, and 44.6 kcal/mol.[20] Specific changes in hydrogen bonding are expected to be important along the reaction path in water, and such effects are not reflected in the simple continuum treatment. To explore this issue further, new calculations on the present system were carried out using the more advanced PCM.[21] Transition structures and reactant geometries were initially located in vacuum at the B3LYP/6-31G* level using Gaussian 03.[19] Single-point energy calculations using B3LYP and MP2 with a larger basis set, 6-311+G(2d,p), were then executed for three different solvents using the PCM method to yield the $\Delta G^{\ddagger}$ results in Table 3.

The computed DFT gas-phase structures are nearly identical to the PDDG/PM3 geometries for the threo and erythro isomers; however, the DFT calculations did predict longer making/breaking bonds at the transition structures with R_{OH} and R_{CN} distances of 1.28 Å and 2.15 Å, respectively, and a little greater emerging double-bond character with a C−C distance of 1.43 Å for the threo reaction (erythro gave similar results). The corresponding results from the PDDG/PM3 calculations are in Table 1. The $\Delta G^{\ddagger}$ values computed with DFT/PCM are underestimated when compared to those from experiment, consistent with the prior finding in the gas phase for the parent system.[20] However, the MP2/PCM results in the aprotic solvents agree very well with experiment, though in all cases the PCM model still seriously underestimates the effect on $\Delta G^{\ddagger}$ in going from the aprotic solvents to water. The QM/MM/MC calculations clearly overcome this problem (Table 2). The results highlight the need for explicit representation of hydrogen bonding in water.

It may be noted that the gas-phase activation enthalpies at 25 °C from the B3LYP and MP2 calculations with the 6-311+G(2d,p) basis set are 13.8 and 18.3 kcal/mol for the threo isomer and 12.5 and 17.0 kcal/mol for the erythro isomer. The corresponding PDDG/PM3 results were again 22.4 and 24.5 kcal/mol. On the basis of the results in Tables 2 and 3, it appears that the MP2 and PDDG/PM3 estimates are quite accurate.

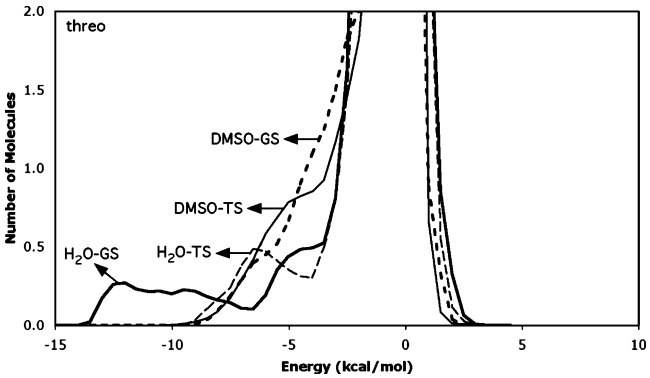

Figure 3. Solute−solvent energy pair distributions for the threo amine oxide elimination in water and DMSO for the reactant (GS) and transition structure (TS) at 25 °C. The ordinate records the number of solvent molecules that interact with the solutes with their interaction energy on the abscissa. Units for the ordinate are number of molecules per kcal/mol.

Solvation. Detailed insights on the changes in solvation along the reaction pathways are available from the QM/MM/MC calculations. In particular, the solute−solvent energy pair distributions record the average number of solvent molecules that interact with the solute and the associated energy. The results for the Cope elimination in water and DMSO for the threo isomer are shown in Figure 3; the results for THF and the erythro isomer can be found in the Supporting Information. Hydrogen bonding in water and the most favorable interaction energies in aprotic solvents are reflected in the left-most region, with energies more attractive than ca. −5 kcal/mol. The large bands near 0 kcal/mol result from the many distant solvent molecules in outer shells. It is immediately clear in viewing Figure 3 that there is much greater loss in very favorable solute−solvent interactions for water than DMSO in proceeding from the reactants to the transition structure. The low-energy band in water for the reactant arises from hydrogen-bond donation to the oxygen of the amine oxide; these interactions diminish significantly for the transition structure as the oxygen takes on hydroxyl character. Integration of the bands from −15 to −4.5 kcal/mol yields four water molecules for the reactant and three for the transition state, and the average strength weakens from ca. −10 to −7 kcal/mol. From display of configurations such as in Figure 4, on average there are three short, strong O···H hydrogen bonds with water molecules for the reactant and one to two longer, weaker ones for the transition structure. The remaining strongly attractive interaction is for a π-type hydrogen bond with the phenyl rings. The stabilization from O···H hydrogen bonding is reduced at the transition structure due to diminished steric accessibility of the oxygen and to charge delocalization compared to that of the reactant (Figure 5). In particular, the strongly dipolar character of the N and O of the amine oxide (+0.68, −0.78 e) is lost in the transition structure (+0.07, −0.54 e).

Large differences are found between the energy pair distributions for water and the polar aprotic solvents (Figure 3 and the Supporting Information). The low-energy bands for the aprotic solvents reflect less favorable interactions compared to those of the strong hydrogen bonds in water. Integration of the bands from −10 to −4.5 kcal/mol yields three to four DMSO molecules for both the reactant and transition state with little

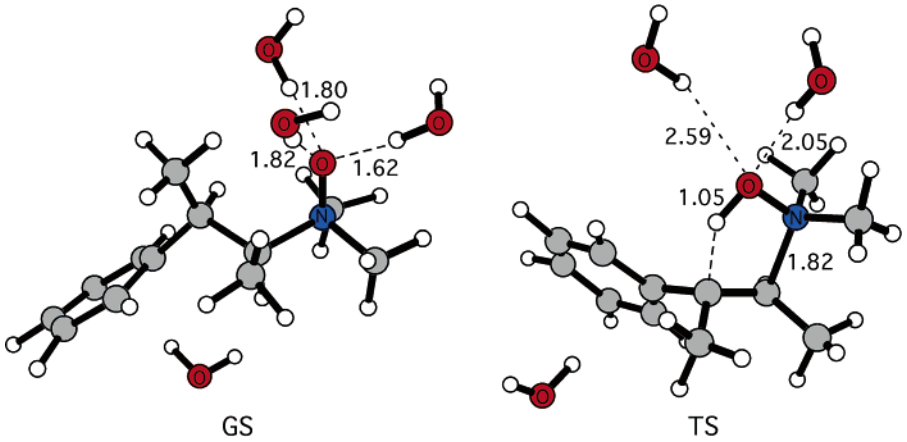

Figure 4. Typical snapshot for the reactant (GS) and transition structure (TS) for the reaction of *threo-N,N*-dimethyl-3-phenyl-2-butylamine oxide in water (only nearest water molecules are illustrated). Distances are in angstroms.

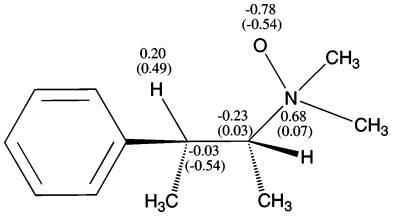

Figure 5. Selected atomic CM3 charges for the ground state and transition structure (in parentheses) for the reaction of *threo-N,N*-dimethyl-3-phenyl-2-butylamine oxide in water using PDDG/PM3.

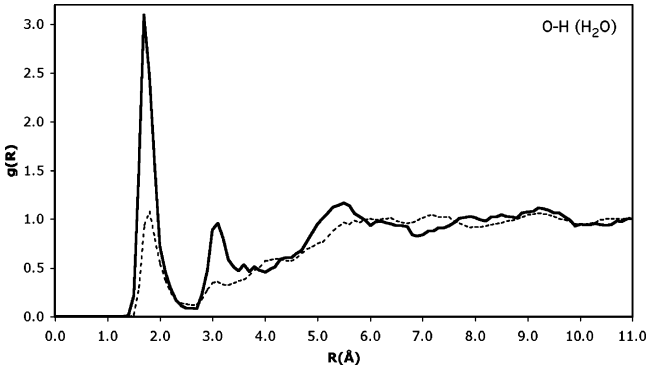

Figure 6. Computed (amine oxide)−O···H−(water) radial distribution functions for the reactant (solid curve) and transition state (dashed curve) for the reaction of *threo-N,N*-dimethyl-3-phenyl-2-butylamine oxide at 25 °C.

shift in the average interaction energy. The dipole−dipole interactions are simply weaker and less specific than the hydrogen bonding with water. Even solvation of the charge-delocalized transition state is more favorable in water with a band centered around −7 kcal/mol, while in DMSO the center of the band shifts to about −5 kcal/mol. The principal contributor to the enhanced rates in the aprotic solvents clearly arises from reduced stabilization of the reactant compared to that provided by hydrogen bonding in water.

It may be noted that Sahyun and Cram explored the strength of the hydrogen bonding between water and the amine oxides through their kinetic studies.[3] A linear relationship between the free energy of activation and mol % of water in DMSO allowed them to estimate the free-energy change for forming a hydrogen bond between water and the amine oxide to be −7 kcal/mol. This value is generally consistent with the range of hydrogen-bond interaction energies that are represented by the lowest-energy band in Figure 3.

The solute−solvent structure for the reactants and transition states in water and the aprotic solvents can be further characterized by radial distribution functions, $g(R)$. In water, hydrogen bonds between the oxygen of the amine oxide and the hydrogens of water, (amine oxide)−O···H−(water), should be reflected in contacts shorter than 2.5 Å. The corresponding $g(R)$ gives the probability of finding the H on water at a distance R from the oxygen of the amine oxide. The expected loss of hydrogen bonding between water and the threo amine oxide during the Cope elimination is apparent in Figure 6, as the reactant progresses to the transition state. The centers of the first peak in the (amine oxide)−O···H−(water) radial distribution functions are at 1.7 and 1.8 Å for the reactant and transition state, respectively; however, the striking first peak for the reactant is significantly reduced at the transition structure, as expected from Figures 3−5. Integration of the first peaks to the minima near 2.5 Å reveals averages of 3.0 and 1.5 hydrogen bonds between the amine oxide oxygen and water molecule for the reactant and transition structure. The latter is consistent with the existence of two similarly populated geometries with either one or two hydrogen-bond donating water molecules. In the right-hand snapshot in Figure 4, there is one strong hydrogen bond and one long one. It may also be noted that in what appears to be the only prior MC or molecular dynamics simulation for an amine oxide in aqueous solution, the number of hydrogen-bonded water molecules was found to be 2.5 at 65 °C.[7]

The interactions between the united-atom CH_3 group on DMSO and the oxygen of the amine oxides, (amine oxide)−O···CH_3−(DMSO), were also explored using radial distribution functions for the reactant and transition structures (Figure 7). Consistent with Figure 3, the differences between the reactant and transition structure are much diminished in comparison to the results for water. Also, the shortest C−O contacts have now been pushed out to 3−4 Å versus 2−3 Å for O−O (amine oxide−water) contacts.

Conclusions

QM/MM/MC simulations have been carried out for Cope elimination reactions with good success in reproducing experimentally observed free energies of activation in water, THF, and DMSO. The overall quantitative success supports the utility of the present QM/MM/MC approach using PDDG/PM3 as the

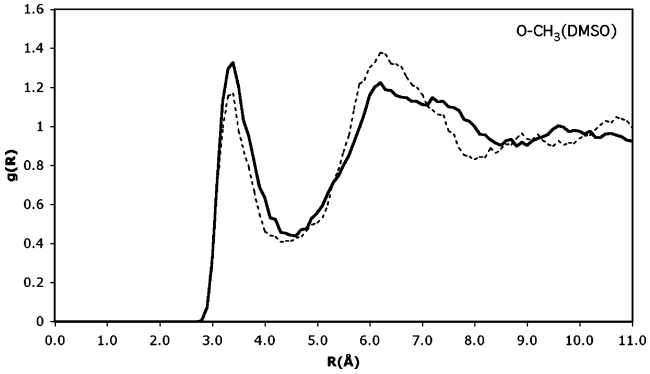

Figure 7. Computed (amine oxide)−O···CH_3–(DMSO) radial distribution functions for the reactant (solid curve) and transition state (dashed curve) for the reaction of *threo-N,N*-dimethyl-3-phenyl-2-butylamine oxide.

QM method. Coupled with the prior success for S_N2, S_NAr, and Kemp reactions, strong encouragement has been provided for further utilization of this methodology for both organic and enzymatic reactions. The importance of the representation of explicit solute−solvent interactions along the reaction path is evident in energy pair distributions, radial distribution functions, and in the failure of QM/continuum models to reproduce the large rate decrease observed for the Cope eliminations in water. Consistent with normal expectations for solvent effects on organic reactions, the rate retardation for Cope eliminations in protic solvents was confirmed to arise from preferential hydrogen bonding with the amine oxide.[22] The present computations have enriched this knowledge with new details (Figures 3−7); notably, the oxygen of the amine oxide accepts three strong hydrogen bonds for the reactant and one to two weaker ones at the transition state in water. Such information can be exploited in the design of catalysts.[23]

Acknowledgment. Gratitude is expressed to the National Science Foundation (CHE-0130996) and the National Institutes of Health (GM032136) for support of this research.

Supporting Information Available: Additional energy pair distributions and radial distribution functions for the Cope eliminations. This material is available free of charge via the Internet at http://pubs.acs.org.

JA057523X

(22) Reichardt, C. *Solvents and Solvent Effects in Organic Chemistry*, 3rd ed.; Wiley: Weinheim, Germany, 2003; p 261.
(23) Curran, D. P.; Kuo, L. H. *Tetrahedron Lett.* **1995**, *36*, 6647−6650.